Recent developments in the design of nanomaterials for photothermal and magnetic hyperthermia induced controllable drug delivery

Alexander E. Dunn,[a] Douglas J. Dunn,[a] May Lim,*[a] Cyrille Boyer[b] and Nguyễn Thi Kim Thanh[c]

DOI: 10.1039/9781849737623-00225

Recent developments in anti-cancer drugs are focused on minimising side effects and improving treatment efficacy. This can be achieved by using a carrier that releases the drug in response to a stimulus. In recent years, research has been directed towards the use of light or alternating magnetic fields as remote stimuli in what is called photothermal and magnetic hyperthermia induced controllable drug delivery, respectively. Much progress has also been made in the use of nanoparticles and polymeric macromolecules as drug carriers. By combining polymers with inorganic nanoparticles into a single entity, it becomes possible to harness the light or magnetic field responsive properties of nanoparticles with the drug storage and release properties of polymers for drug delivery. In this review, we explore recent developments of polymer-nanoparticle hybrids drug carriers for photothermal and magnetic hyperthermia controllable drug delivery.

1 Introduction

Recent improvements in cancer treatment have resulted in an increase in post-diagnosis life expectancy. These improvements were enabled by the development of potent therapeutic agents with novel modes of action. Nonetheless, due to their inherent toxicity, many of these therapeutic agents are limited by the dose that can be safely delivered without causing debilitating side effects. In addition, a systemic route of administration often results in a narrow therapeutic window such that prolonged exposure to the therapeutic agent is required in order to achieve sufficient treatment efficacy. This may lead to indiscriminate cytotoxicity of the therapeutic agent toward normal and cancer cells throughout the body, resulting in severe side effects such as immunosuppression and organ failure in the patient.

A nanomaterial based controllable drug delivery platform would overcome many of the major drawbacks in cancer therapy. These nanocarriers store the therapeutic agent in an inert and protected state during transportation and subsequently provide concentrated and on-demand release of

[a]*ARC Centre of Excellence for Functional Nanomaterials, School of Chemical Engineering, The University of New South Wales, Sydney NSW 2052, Australia*
[b]*Australian Centre for NanoMedicine and Centre for Advanced Macromolecular Design, School of Chemical Engineering, The University of New South Wales, Sydney NSW 2052, Australia*
[c]*Department of Physics and Astronomy, University College London, Gower Street, WC1E 6BT, London, United Kingdom and UCL Healthcare Biomagnetic and Nanomaterials Laboratories, 21 Albemarle Street, London, W1S 4BS, United Kingdom.*
**E-mail: m.lim@unsw.edu.au*

the agent at the site of the cancer.[1–5] In particular, the ability to control the timing, dosage and release profile of the agent as well as being able to carry out repeated on-demand dosing from a single administration would greatly increase the efficacy of the therapeutic agents. The short and long-term damage to healthy tissue will also be minimised. This approach may also help address the importance of timing on therapeutic effects, such as chrono-administration, a new concept that is receiving increasing recognition.[6]

Controlled release of drugs from a nanocarrier can be facilitated by either a local or remote stimulus. A local stimulus is one that relies on changes in conditions within the body, often taking advantage of physical and/or chemical characteristics that are unique to diseased tissue to release the drug from the carrier. A remote stimulus is one that exists outside the body, and ideally, should be non-invasive, non-irradiative, and yet able to penetrate the body for localised drug release. Remote stimuli are of particular significance because they can provide both temporal and spatial control over the drug release.

The use of light or an alternating magnetic field as remote stimuli for the controllable release of drugs, in what is known respectively as photothermal and magnetic hyperthermia induced controllable drug release, has gained much interest recently. In magnetic hyperthermia induced drug release, the drug carrier would consist of a magnetic nanomaterial that interacts specifically with an oscillating magnetic field.[7] Photothermal induced drug release relies on the interaction between a plasmonic nanomaterial and visible or infrared light.[8] Typically these interactions result in the generation of heat within the nanocarriers, which in turn initiates release of the drug. Herein, we will review recent developments in the design of nanomaterials for magnetic hyperthermia and photothermal induced controllable drug delivery, focusing on organic-inorganic hybrid systems. We will provide an overview of different ways in which metallic or oxide nanomaterials can be conjugated with polymeric macromolecules to facilitate photothermal and magnetic hyperthermia induced controllable drug delivery. Thereafter, we will review recent developments in photothermal and magnetic hyperthermia induced drug release.

1.1 Organic-inorganic hybrid nanomaterials for photothermal or magnetic hyperthermia induced controllable drug delivery

1.1.1 Design of nanomaterials for photothermal and magnetic hyperthermia induced controllable drug delivery. Stimulus responsive nano drug carrier platforms can be broadly categorized as organic-based, inorganic-based or a hybrid combination of the aforementioned. Inorganic nano-platforms include metallic nanoparticles (*e.g.* gold, silver), oxides (*e.g.* iron oxides, silica), and quantum dots. Organic nano-platforms include polymeric nanoparticles, micelles, liposomes, polymersomes and dendrimers. The use of carbon-based nanomaterials (*e.g.*, fullerenes, carbon nanotubes and graphene) has also been explored recently, although questions have been raised regarding the biocompatibility of these materials. Examples of hybrid platforms include colloidal gold encapsulated in liposomes and superparamagnetic iron oxide particles with polymer-grafted surfaces.

The most commonly reported structures for photothermal and magnetic hyperthermia induced controllable drug delivery are outlined in Fig. 1. Most of these structures are derived from earlier designs of nanomaterials based drug carriers. Perhaps the most significant of these developments was the combination of organic and inorganic materials; specifically, the light or magnetic field responsive properties of the inorganic nanomaterials were combined with the drug loading and release properties of the organic macromolecules to yield composites with controllable drug delivery capabilities.

Inorganic nanostructures for the purpose of photothermal and hyperthermia induced drug delivery almost exclusively incorporate two or more nanomaterials, whereby each provides specific functionality. The simplest designs involve the encapsulation of light or magnetic responsive materials (*e.g.* plasmonic gold nanorods for photothermal heating and magnetite nanoparticles for magnetic) within a mesoporous shell structure (see Fig. 1a), or decoration of the mesoporous structure's surface with the stimuli responsive nanoparticles (see Fig. 1b). The most commonly used mesoporous compound is silica, due to the facile synthesis methods (usually

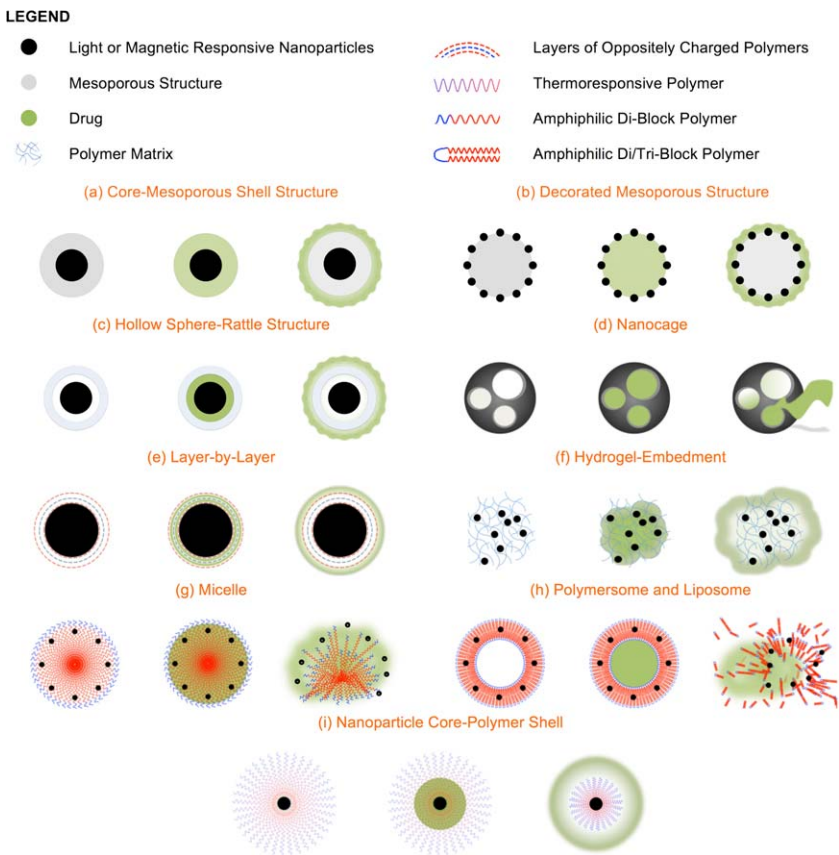

Fig. 1 Visual representation of the structure (left), loading of drug (centre) and release of drug (right) for the commonly used nanostructures in photothermal and magnetic hyperthermia induced controllable drug delivery.

via the well-established Stöber method).[9] In these carriers, the drug is stored within the pores of the mesoporous material[10–12] and released upon thermal expansion; this heat is generated by the interactions between the light and plasmonic nanomaterials, or between the alternating magnetic field and magnetic nanomaterials. Whilst simple to fabricate, the functionality of these carriers is usually limited by a low storage capacity. That is, it is usually not possible to deliver a meaningful quantity of the drug due to the small storage volume of the pores in the mesoporous material and the poor absorptivity of some drugs onto the carrier.

To address this issue, some groups have investigated the use of hollow spheres-rattle structures, in which the 'rattle' is a light responsive or magnetic material (see Fig. 1c).[13,14] These structures improve drug-loading capacity by integrating additional storage space through means of a hollow interior, and the mesoporous shells provide a pathway for diffusion of the drug from the interior of the carrier. It is noted here that most methods for synthesising inorganic hollow sphere with rattle structures are not trivial. It is only with the development of facile synthesis methods in 2008 and 2009 (for instance the work of Yin and co-workers) that the use of hollow spheres with rattles structure has become feasible for controllable drug delivery.[15–18]

Another recent development is the use of nanocages for photothermal induced drug delivery. Nanocages are hollowed out nanoparticles with a cage-like surface structure, in which the porous material and the stimulus responsive material are one and the same (see Fig. 1d). The storage and release of drug from the nanocage is facilitated through the inclusion of a phase change material that traps the drug within the nanocage until release is initiated by a temperature change. Gold nanocages have been constructed by first forming a gold-silver alloy nanoparticle, followed by etching of the silver to obtain the cage-like structure.[19,20]

Each of the aforementioned inorganic nanostructures has a number of significant design limitations. Firstly, most of them rely on diffusion as the main mechanism for drug release. Diffusion of the drug is driven by concentration gradients between the interior and exterior of the drug delivery agent. While the rate of diffusion may be modified to some extent by introducing a physical barrier or altering the environment of the drug carrier, a driving force for diffusion will always be present. This results in premature release of the drug from the carrier, as well as a lack of control over the drug release rate and profile. Secondly, some of these inorganic nanostructures lack *in vivo* stability and biocompatibility; for *in vivo* applications, aggregates of nanoparticles that are larger than 4 μm can disrupt blood flow through veins or capillaries.[21] Large nanoparticles are also more likely to be captured and removed by the reticuloendothelial system (RES); this is reflected by a short retention time of the drug carrier in the body. This is generally a suboptimal phenomenon because sufficient retention time of the drug carrier is required if meaningful quantities of drug are to be released.

To address these three issues, researchers have considered the use of polymeric macromolecules. Polymers have been shown to improve size stability, increase residence time, and enhance the permeability and retention of nanoparticles in cancer cells through provision of charge and

steric repulsions. In addition, polymeric compounds have also been shown to facilitate drug storage by providing a chemical or physical adhesion mechanism. Some of the earliest demonstrations of photothermal and magnetic hyperthermia induced drug delivery are from organic-inorganic nanocomposites prepared *via* the Layer-by-Layer (LbL) and hydrogel-embedment approaches.[22,23] In the LbL method, the drug carrier consists of a nanoparticle core that is coated in alternating layers of positively and negatively charged polymers, with the drug trapped between each layer (see Fig. 1e). The polymer layers are held in place by electrostatic forces from the oppositely charged layers before and after it. In the embedment structure, the drug carrier consists of a network of cross-linked polymer networks, sometimes referred to as a hydrogel, with the drug adsorbed within the gel matrix (see Fig. 1f). In both cases, the drug is weakly associated with the drug carrier and can be released in response to changes in pH, ionic strength, or in the case of photothermal and magnetic hyperthermia induced drug release, a change in temperature. For photothermal and magnetic hyperthermia induced drug release from the LbL and hydrogel/embedment constructs, heat is generated by plasmonic or magnetic nanoparticle cores that respond to light and alternating magnetic fields, respectively.

These electrostatic interaction based methods for modifying inorganic materials with polymers also suffer from low drug storage capacity and limitations associated with the type of drug that can be stored. To address this, researchers have developed a family of organic vesicle structures that can be broadly categorised as micelles, liposomes and polymersomes. These structures are composed of amphiphilic macromolecules: phospholipids in the case of liposomes, and amphiphilic di- or tri-block copolymers in the case of micelles and polymersomes. Micelles are formed when the amphiphilic polymers align to form a spheroid with a hydrophobic core (see Fig. 1g). Liposomes and their synthetic counter-part, polymersomes, are formed when the polymers self-assemble to form a hydrophobic bilayer membrane that encapsulates a hydrophilic core (see Fig. 1g).[24,25] The key advantages of these vesicle structures are their large drug storage capacity and the capability to load hydrophobic drugs. Moreover, for liposomes and polymersomes, hydrophobic and hydrophilic drugs can be dissolved into the bilayer membrane and central cavity, respectively, thus enabling drugs with different polarities to be delivered within a single nanostructure. The stability of these vesicle structures is dependent on the conditions of the surroundings such as pH, ionic strength and temperature. Thus, by incorporating stimuli responsive nanoparticles that are able to induce a change in the local surroundings, it is possible to induce drug release at a desired time and location in response to the stimulus applied by the administering clinicians.

Carriers that are based on electrostatic interactions between the polymer and inorganic particles also rely on the fact that the polymer can adsorb onto the particle core; these designs further assume that the polymer layers do not detach with changes to the environment pre-drug delivery and release. Where these conditions cannot be met, a better method for conjugating polymer to nanoparticle would be one where the polymer is chemically bonded to the particle to form a nanoparticle core-polymer shell

structure (see Fig. 1i). For applications in photothermal and magnetic hyperthermia induced drug release, the design typically incorporates a temperature responsive polymer that is conjugated to a light or magnetic responsive nanoparticle core, respectively. When heat is generated by the photothermal or magnetic hyperthermia effects, the polymer will contract in a manner that results in the release of drug from the drug carrier.

Evidence outlined herein seems to indicate that organic-inorganic hybrid nanomaterials are currently the most promising carrier for controllable drug delivery. The strength of these nanocarriers lies in their ability to improve functionality by harnessing the beneficial properties of both the inorganic and organic components. Typically, the inorganic component provides a stimulus response mechanism, while the organic component improves *in vivo* stability, biocompatibility and provides a drug storage/release mechanism. In the following section we will examine the key considerations for the design of these polymers and the various methods for organic-inorganic nanomaterial conjugation. We will also look at the ways in which the properties of the polymer may be tailored to suit the desired drug storage properties of the nanocomposite.

1.1.2 Strategies for polymer design and organic-inorganic nanomaterial conjugation. As outlined in the previous section, polymers play a key role in improving the size stability, biocompatibility, uptake, retention and drug storage capacity of most nanomaterial based drug delivery platform.[26–29] The main designs of interest are nanoparticle core-polymer shell and polymeric vesicles. Herein, we outline the ways in which the polymer is designed, and subsequently conjugated to the inorganic nanomaterials to form an efficient interdependent mechanism that can be used for controllable drug delivery.

Design of polymers

The key considerations in the design of a nanoparticle based drug delivery platforms for *in-vivo* applications are:

(i) The nanoparticles should be present in a size range between 10 nm to 200 nm, to take advantage of the enhanced permeability and retention (EPR) effect[30–32] that is caused by an increased permeability of the vascular system and inefficient lymphatic drainage close to tumour sites;

(ii) The surface of these nanoparticles should be anti-fouling to avoid rapid absorption of proteins, and therefore limit their clearance by the reticuloendothelial system; and[33]

(iii) The colloidal stability of the nanoparticles should be maintained in biological fluid to avoid aggregation and precipitation.

Each of these objectives may be achieved by coating the inorganic nanoparticles with a polymer. A polymer coating provides colloidal stability in water through steric stabilisation, and can provide surface functionality allowing the possibility of designing hybrid particles with capacity for multimodal targeting. In addition, the polymer shell can be employed to encapsulate therapeutic compounds thus providing the possibility of controlled release.[27]

The first generations of polymers used for the stabilisation of inorganic nanomaterials were based on natural polymers, such as dextran or carbohydrate derivatives. These biopolymers were adopted for their ability to interact with iron oxide nanoparticle surfaces whilst simultaneously conferring stability in blood plasma. Since then, a number of more advanced polymer designs have since been considered; polyvinylpyrrolidone (PVP), polyvinyl alcohol (PVA), polyethylene glycol (PEG) and its meth(acrylate) derivatives, poly(hydroxypropyl methacrylamide), and poly(*N*-acryloylmorpholine)[33] are among the most widely investigated.[34–37] These polymers are generally deemed 'biocompatible', although it is important to note that both PVA and PVP can adversely adsorb proteins because of H-bonding interactions.[38]

Further advancements in polymer synthesis techniques (using controlled radical polymerisation) have enabled the design of highly customisable polymers with well-controlled properties. For instance, an alternative to the generic linear polymer chains is the use of brush polymers (and copolymers) of poly(oligoethylene oxide (meth)acrylate).[33,39–42] These brush-like polymers (short PEG chains grafted onto an acrylic backbone) offer comparable anti-fouling properties and blood compatibility to linear PEG.[39]

In addition, polymers may be designed to be responsive to a change in their environment, such as pH, temperature and light.[43–48] These physical changes can be exploited in drug delivery to control the release profile of therapeutic agents. Temperature responsive polymers are the most relevant for photothermal and magnetic hyperthermia induced drug delivery. Of the thermoresponsive polymers, poly(*N*-isopropylacrylamide) (PNIPAM) is the most widely used due to its easily tuneable thermoresponsive properties.[49,50] The lower critical solution temperature (LCST) of PNIPAM is typically around 32 °C, and through copolymerisation with appropriate monomers, such as *N,N'*-dimethylacrylamids and *N*-hydroxymethylacrylamide, this LCST may be manipulated.[47,51,52] The other major advantage of PNIPAM is its affinity to a large range of therapeutic drugs. PNIPAM has been proven to be effective for storage and delivery of several different kinds of model drugs, including heteropolyacids (HPAs),[12] vitamin B_{12},[53] and doxorubicin.[48]

Polymer grafting onto inorganic nanoparticles

In the simplest case, physical attractions between the polymer and nanoparticles can be achieved *via* van der Waals and acid–base interactions, and/or attractive electrostatic interaction between oppositely charged nanoparticles and polymers. This can be achieved through the use of block or random copolymers; these polymers may be enhanced with several functional groups that provide multiple attachment points between the polymer and particle surface.

A more reliable way to conjugate the polymer chains with the nanoparticles is *via* chemical bonds, in what is termed 'grafting'. This is usually achieved through one of two alternative approaches: grafting "onto" and "from".[27] In the grafting "onto" approach, a functional, pre-formed polymer is grafted *in-situ* onto the nanoparticle surface using functionality capable of binding to the inorganic nanoparticles surface. For oxide

nanoparticles such as iron oxide, titanium oxide, cerium oxide, many different types of anchoring groups (dopamine,[54] carboxylic acid,[55] thiol, amine and trimethyl silane[56]) can be used.[57–59] The stability of these hybrid organic-inorganic nanoparticles depends on the strength of the affinity between the anchoring group and the oxide surface. Thiol and amine groups do not provide strong interaction with oxide inorganic materials, thus limiting their feasibility for bio-application, whilst carboxylic acid groups can be displaced by small organic carboxylic acid compounds present in biologic fluid and are limited to a specific range of pH. Multi-carboxylic acid groups have also been introduced to anchor polymers on inorganic nanomaterials.[60] A sturdier alternative is the use of silane groups that can be covalently attached onto the oxide surface by reaction of the oxide layer (*e.g.* Metal-OH) with the silane group. De Palma and co-workers[61] shows that the silane approach allows stable hybrid iron oxide nanoparticles in a large pH range, to be routinely synthesized. Phosphonic acid groups are also commonly exploited to anchor polymers onto different oxides; this often yields stability in a large range of pH and salt media. For metallic nanoparticles such as gold or silver, thiol or disulphide bonds can be employed to covalently attach polymers to the surface. For example, Haddleton[62,63] and other groups[33,64] have demonstrated that thiol presents a very strong affinity to gold surfaces, which in turn allows us to produce gold nanoparticles that are stable in biologic fluid.

In the case of grafting "from", an initiator molecule is fixed to the surface of the nanoparticle and the polymer is grown from the surface.[41] Different polymerisation techniques have been employed to achieve this: initially living anionic/cationic polymerisations, and more recently, controlled radical polymerisation, such as reversible addition fragmentation transfer polymerisation,[65] atom transfer radical polymerisation,[41,66,67] and nitroxide mediated polymerisation.[68] The use of these recent controlled radical polymerisation techniques has allowed us to tailor the polymer structures and to control a large range of functional monomers.[69]

As to whether grafting "from" or grafting "onto" is the better approach, the general consensus is grafting "from" yields a higher grafting density than the grafting "onto" approach.[41,70] However, grafting "onto" allows better control of polymer architecture and functionality, and is therefore more versatile than the grafting "from" method. In addition, grafting "from" can present difficulties in maintaining the colloidal stability of the hybrid nanoparticles in organic solvents. Nonetheless, the use of living radical polymerisation, with a carefully designed protocol, has been achieved for the modification of nanoparticles using the grafting "from" approach. For example, Hatton *et al.*[71] grafted several polymers from iron oxide nanoparticles coated with ATRP initiator. Ring opening polymerisation has also employed to obtain iron oxide nanoparticles coated with linear biodegradable poly(esters)[72] or by hyper-branched polymers.[73]

An alternative approach to grafting "onto" or "from" has been proposed using the recent development of high yield "click chemistries" (*e.g.* azide-alkyne[74,75]). These reactions provide further alternative routes to functionalising nanoparticles with polymers. For example, Turro *et al.*[76] described the stabilisation of maghemite nanoparticles using alkyne

terminated organophosphate or carboxylic acid groups to exchange with oleic acid on the iron oxide's surface. The maghemite particles were subsequently covalently attached to poly(*tert*-butyl acrylate) *via* click reactions using $CuSO_4$ as the catalyst.

Drug loading

A number of recent studies have shown that it is also possible to utilise polymers to encapsulate drugs *via* hydrophobic/electrostatic interactions or covalent bonds. Initial studies employed the use of electrostatic or hydrophobic interactions to trap drugs in a polymer matrix, or within the vesicles of micelles and polysomes/liposomes. It is important to note that in these structures, the slow diffusion of the therapeutic compounds from the polymer into the surrounding area may still occur, resulting in unspecific delivery. As an alternative approach, researchers developed labile linkers to connect therapeutic drugs to the polymer, providing a more sturdy bond and greater control over the delivery mechanism.[77–79] The breakage of these bonds can be triggered by an internal or external stimulus. For example, Yamashita *et al.* (2011) examined the use of a heat-labile, double stranded oligonucleotide as a linking agent between a gold nanorod and a PEG chain. Yamashita suggested that heat induced by the photothermal effect could be harnessed to sever this covalent bond by a retro Diels-alder reaction.[80,81]

2 Photothermal induced drug release

Light is used in photothermal induced drug release to cause a plasmonic nanomaterial to heat up, which in turn activates a heat-responsive drug release mechanism. This concept originated, in part, from photothermal therapy (also known as photoablation therapy) and photodynamic therapy, where light is used to generate heat and activate a photo-sensitive drug, respectively, in diseased cells. By itself, photothermal therapy rarely has the ability to completely destroy diseased cells and is thus never used as the sole mode of treatment.[82] Instead it is used in conjunction with other techniques such as chemotherapy, in which the heat that is released causes the pores of the diseased cells to expand, thereby improving the uptake of therapeutic drugs. Thus, applying the photothermal effect to controllable drug delivery, where the drug that is conjugated to plasmonic nanomaterial by a heat-responsive polymer, and released in response to heat from the photothermal effect, is a logical extension.

Gold nanoparticles form the basis of recent research into photothermal induced controllable drug delivery due to their established method of production, well-understood chemistry and low toxicity towards biological cells as seen in many *in vivo* and *in vitro* studies.[83] When irradiated with light, electrons in the conduction band of the gold nanoparticle are excited, followed by intraband decay of the electrons. This results in a conversion of light energy to thermal energy in what is referred to as localized surface plasmon resonance.[84–86] The ease with which gold nanoparticles can be modified to have specific peak absorbance in the visible to near-infrared region (400 nm to 1100 nm) is another reason why they are attractive for photothermal drug release applications. For *in vivo* applications, light in the

visible to infrared wavelength range is favoured due to the fact that they are less energetic and therefore less harmful to cells and tissues. Infrared light is also less attenuated by human tissue, thus enabling penetration of up to 1 cm for subcutaneous treatment.[87]

2.1 Recent developments in the application of nanomaterials for photothermal induced drug release

2.1.1 Design and synthesis of nanomaterials for photothermal applications. Gold nanospheres and gold nanorods are the most widely investigated gold nanostructures for photothermal induced drug release; this is due to their well-established methods of production and well-understood chemistry. Recent investigations have shifted focus to conjugates of gold nanospheres and nanorods with polymers, as well as other gold nanostructures. More complex morphologies such as gold vesicles (a spherical, densely packed, monolayer gold nanoparticle shell tethered using amphiphilic block copolymers),[88] nanoshells and half-shells,[1,94] nanocages[19] and nanostars[95] have been proposed for photothermal applications due to their increased surface area or loading capacity (see Fig. 3). Some investigators have also explored the use of material other than gold as photothermal agents.

An *et al*. developed 150 nm to 200 nm size thermo-sensitive liposomes with hydrophobic gold nanoparticles embedded within the liposome bilayer and the drug berberine encapsulated within the liposome's compartment (see Fig. 2).[89] This agent was prepared using the film build method in combination with supercritical CO_2 incubation, which permits the size and stability of the liposomes to be controlled by adjusting the preparation pressure. Ultraviolet light (250 nm) was used to induce the photothermal effect, and release of over 50% of the berberine within 5 min was demonstrated. This drug release rate is unprecedented, and correlates with the amount of embedded gold nanoparticles. Commutative irradiation using ultraviolet and visible light further shows that the photothermal effect induces phase transition in the liposomes without destroying the bilayer structure. The stability and the drug encapsulation efficiency of the liposome was found to decrease with increasing amounts of gold nanoparticles

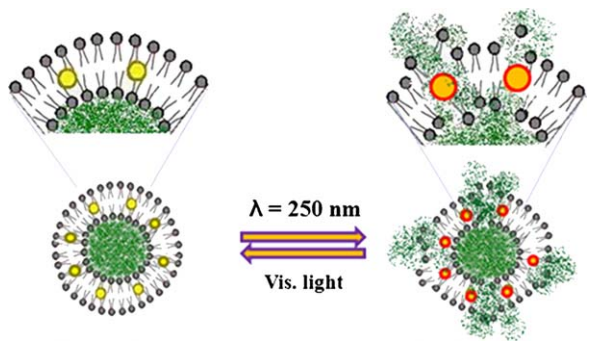

Fig. 2 Gold nanoparticle-liposomes conjugate drug release *via* light irradiation.[142] Reprinted with permission from X. An, F. Zhan and Y. Zhu, *Langmuir*, 2013, **29**, 1061–1068. Copyright 2013 American Chemical Society.

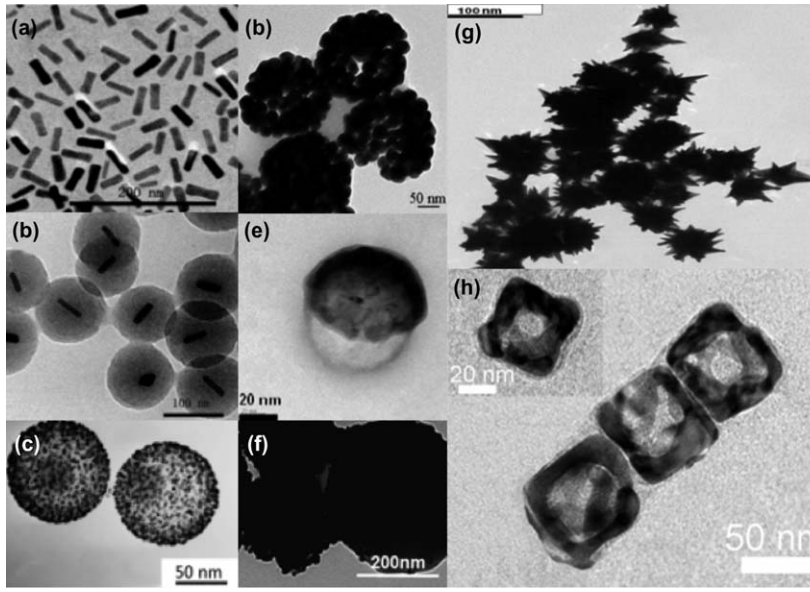

Fig. 3 TEM images of (a) gold nanorods,[100] (b) silica encapsulated gold nanorods,[100] (c) gold decorated silica rattle structure,[99] (d) gold vesicles,[88] (e) gold nano half-shell,[105] (f) gold nano shells,[1] (g) nanostars[92] and (h) nanocages.[143] Reprinted with permission from Z. Jiang, B. Dong, B. Chen, J. Wang, L. Xu, S. Zhang and H. Song, *Small*, 2013, **9**, 604–612. Copyright (2013) John Wiley and Sons. H. Liu, D. Chen, L. Li, T. Liu, L. Tan, X. Wu and F. Tang, *Angewandte Chemie International Edition*, 2011, **50**, 891–895. Copyright (2010) John Wiley and Sons. J. Lin, S. Wang, P. Huang, Z. Wang, S. Chen, G. Niu, W. Li, J. He, D. Cui, G. Lu, X. Chen and Z. Nie, *ACS Nano*, 2013, **7**, 5320–5329. Copyright (2013) American Chemical Society. S.-M. Lee, H. J. Kim, Y.-J. Ha, Y. N. Park, S.-K. Lee, Y.-B. Park and K.-H. Yoo, *ACS Nano*, 2012, **7**, 50–57. Copyright (2012) American Chemical Society. Y. Ma, X. Liang, S. Tong, G. Bao, Q. Ren and Z. Dai, *Advanced Functional Materials*, 2013, **23**, 815–822. Copyright (2013) John Wiley and Sons. Z. Fan, D. Senapati, A. K. Singh and P. C. Ray, *Molecular Pharmaceutics*, 2012, **10**, 857–866. Copyright (2012) American Chemical Society. L. Gao, J. Fei, J. Zhao, H. Li, Y. Cui and J. Li, *ACS Nano*, 2012, **6**, 8030–8040. Copyright (2012) American Chemical Society.

introduced in the preparation step; this was attributed to disruption of the bilayer microstructure of liposomes.

Huang *et al.* shows the photothermal effect can be used to trigger the controlled release of rhodamine 6G (R6G) dye that was incorporated into layer-by-layer assembly of negatively charged poly(acrylic acid, sodium salt) (PAA) and positively charged poly(allylamine hydrochloride) (PAH) polymers on gold nanorods.[90] The drug release was induced *via* heating from a laser that caused the dye to escape through the trapping layers. An increase in the number of trapping layers was shown to decrease the amount of dye released. More interestingly, the release rate is highly dependent on the thermodynamic properties of PAA and PAH, with PAA-only systems showing greater amount of dye molecules bound and a higher release rate. Isothermal titration calorimetry analysis suggested that R6G and PAA have interactions that would favour disassociation of the dye from the polymer upon heating, whereas R6G and PAH showed zero complex formation within the limit of measurement. A capping PAH layer was also shown to bind more tightly to the underlying PAA/R6G layers, thus preventing the dye from being released.

Passive tumour targeting of gold nanocages was assessed by Xia *et al.* [91] and it was found that they are preferentially absorbed by tumour tissue as opposed to normal tissue. These gold nanocages were synthesised *via* a galvanic silver-gold replacement technique where silver nanocubes were initially produced *via* polyol reduction with CF_3OOAg as the silver precursor.[19,20] The silver nanocubes were then mixed in hydrogen tetrachloroaurate which initiated a spontaneous galvanic reaction where the silver underwent dissolution whilst the gold was deposited, eventually forming a nanobox or nanocage with Au-Ag alloying.

Lin *et al.* developed gold vesicles that were loaded with Chlorin e6 (Ce6), a multifunctional photosensitizer.[88] The gold vesicles were obtained *via* the self-assembly of gold nanoparticles tethered with thiol-terminated amphiphilic block copolymers of polyethylene oxide-b-polystyrene in a film rehydration method. The gold vesicles show strong absorbance in the near-infrared range of 650–800 nm due to plasmonic coupling between neighbouring gold nanoparticles in the vesicular membranes. Notably, the gold vesicles showed higher levels of Ce6 loading compared to gold nanorods, as well as excellent biocompatibility, solubility and stability in solution.

Fan *et al.* obtained star shaped gold nanoparticles with a magnetic iron oxide core by dispersing iron oxide nanoparticles in sodium citrate, followed by reduction of hydrogen tetrachloroaurate in the presence of cetyltrimethylammonium bromide and silver nitrate.[92] The nanoparticles were then functionalised with thiolated polyethylene glycol and thiol-modified Cy3-bound S6 aptamers to minimise blood cell interaction, and to enable targeted capture of SK-BR-3 breast cancer cells with a magnet. Controllable drug release was not demonstrated, although photothermal heating was shown to result in cell death. Jing *et al.*[93] worked with polypyrrole coated 'urchinlike' gold nanoparticles. Their study found that the polypyrrole coating improved structural stability of the gold nanoparticles when exposed to heat, pH and laser irradiation and more than doubled their photothermal transduction efficiency.

Zhang *et al.* developed single wall carbon nanotubes that were modified with AS1411 aptamer and loaded with doxorubicin.[94] Carbon nanotubes have previously been shown to have strong optical absorbance in the near infra-red range.[95] In the work of Zhang *et al.*, carbon nanotubes were used to deliver doxorubicin to EC-109 cells due to the AS1411 affinity for nucleolin on the surface of EC-109 cells. While photothermal induced release of drugs was not demonstrated explicitly in Zhang *et al.*'s work, they did demonstrate that photothermal hyperthermia with carbon nanotubes can inhibit the G2-M cell cycle. Similarly, Estrada *et al.*[96] have developed multi-walled carbon nanotubes (MWCNT) functionalised with k-carrageenan hydrogels. In this case, the MWCNTs were employed as a reinforcing agent improving the mechanical properties of the hydrogel as well as a photosensitive material that enabled photothermal delivery.

Another material that has shown potential for photothermal induced drug delivery is graphene. Sahu *et al.* functionalised graphene oxide with poly(ethylene oxide)-poly(propylene oxide)-poly(ethylene oxide) triblock copolymers.[97] The release of methylene blue graphene-polymer conjugate was shown to be pH sensitive and the photothermal effect was shown to

induce cell death. Wang *et al*. developed silica coated graphene nano-sheets functionalised with hydrophilic polyethylene glycol and a targeting peptide (IP) for the delivery of doxorubicin.[98] They showed drug release can be initiated by both pH and temperature.

2.1.2 Photothermal induced controllable drug release. Liu *et al*. developed an all-in-one (photothermal therapy, drug delivery and cell imaging) system based upon silica nano-rattle sphere coated with a gold shell and functionalised with polyethylene glycol for stability.[99] An initial rapid release of Docetaxel (52% loading, approximately 1.08 μg per μg particles) in the first 20 h of drug delivery, followed by sustained release for a period of up to 7 days was observed. *In vivo* and *in vitro* studies showed the combination of photothermal therapy and Docetaxel based chemotherapy has a synergistic effect, which the authors attributed to the altered kinetics, permeability and increase uptake of the drug due to the photothermal process. Interestingly, irradiation by a near infra-red laser light did not result in additional cumulative release of the drug; this was attributed to the good thermal and mechanical stability of the nanocarrier.

Jiang *et al*. have developed mesoporous silica encapsulated gold nanocomposites for use in fluorescence imaging and photothermal controlled drug delivery.[100] Excellent biocompatibility with low toxicity was demonstrated. Additionally photothermal cancer ablation and photothermal drug delivery with doxorubicin were successfully demonstrated *in vitro*.

Gold nanocages have also been used for photothermal induced drug delivery by a phase-change material (PCM) that changes phase from solid to liquid over a very small temperature range. Xia *et al*. demonstrated this drug delivery technology by creating a mixture of doxorubicin immersed in 1-tetradecanol (melting point between 38 and 39 °C), and load the mixture into gold nanocages, whereby the mixture then solidified.[91,101] The photothermal effect could then be used to heat the nanocages and melt the PCM, releasing the drugs. It was found that, for breast cancer cells, this simultaneous drug delivery and photothermal ablation therapy significantly reduced cancer cell viability.

Ma *et al*. developed cholesteryl succinyl silane nanomicelles (CSS) loaded with doxorubicin and magnetite nanoparticles, and coated with a gold shell (see Fig. 4).[1] Using this particle system, they demonstrated this "all-in-one" drug delivery agent allows for photothermal drug release, photothermal therapy, magnetic targeted drug delivery and MR imaging. Irradiation with near-infrared laser was shown to increase the drug release by two-fold and a unique feature of the work is they are able to trigger stepwise release by controlling laser exposure (see Fig. 4). Drug release in the absence of laser irradiation was attributed to the incomplete gold shells. *In vitro* HeLa cell viability tests showed a significant decrease in cell viability only in tests that utilised nanocarriers in conjunction with near infra-red irradiation, thus the effects were attributed to the photothermal release of drug.

Yamashita *et al*.[80,102] demonstrated the *in vivo* release of single strand DNA from double strand DNA-modified gold nanorods that was triggered by the photothermal effect. This work follows their previous *in vitro* studies that showed DNA can be used as a heat-labile linker in photothermal

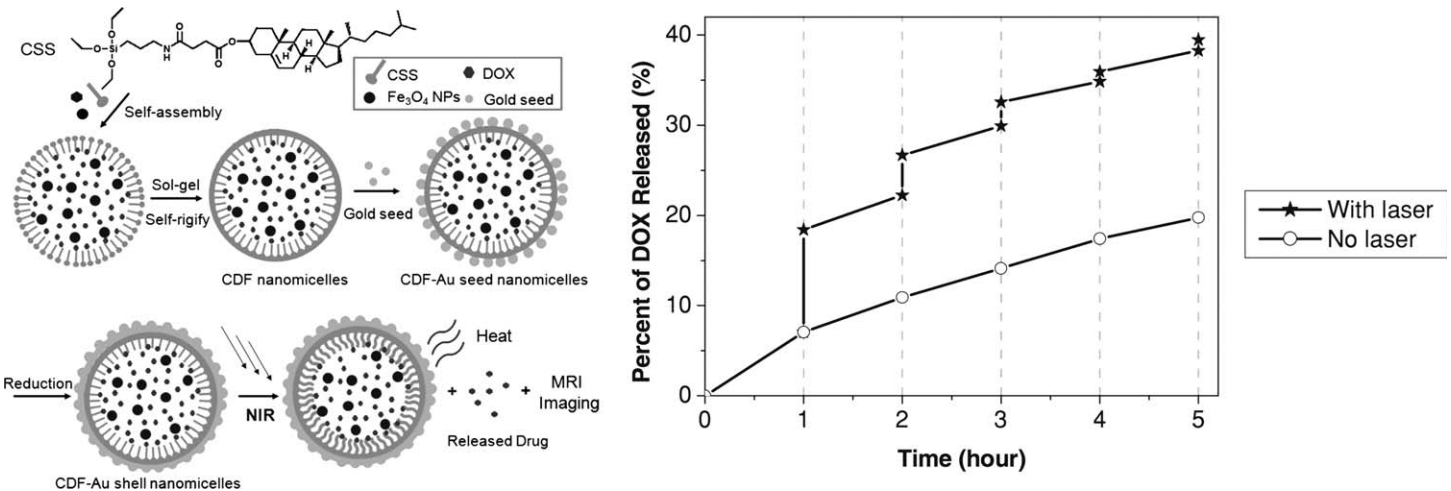

Fig. 4 Schematic showing the fabrication of cholesteryl succinyl silane (CSS) nanomicelles loaded with doxorubicin and magnetite nanoparticles (Fe_3O_4 NPs) and coated with a gold shell (left) and doxorubicin release profile from the nanomicelles in the presence and absence of laser irradiation (right).[1] Reprinted with permission from Y. Ma, X. Liang, S. Tong, G. Bao, Q. Ren and Z. Dai, *Advanced Functional Materials*, 2013, **23**, 815–822. Copyright 2013 John Wiley and Sons.

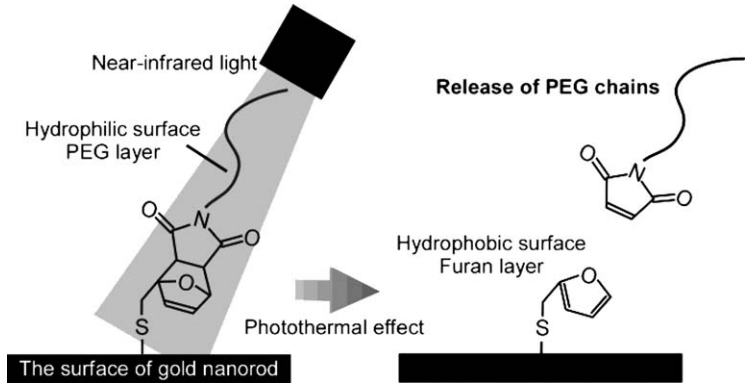

Fig. 5 PEG chain release from gold nanorods due to photothermal effect triggered retro Diels-Alder reaction.[102] Reprinted with permission from S. Yamashita, H. Fukushima, Y. Niidome, T. Mori, Y. Katayama and T. Niidome, *Langmuir*, 2011, **27**, 14621–14626. Copyright 2011 American Chemical Society.

induced release of therapeutics. The same group also showed the controlled-release system of polyethylene glycol polymer from the surface of the gold nanorods triggered by a retro Diels-Alder reaction induced by the photothermal effect (see Fig. 5).

Zanberg *et al*. demonstrated the release of smaller fluorescent dye molecules from 16 nm gold or 200 nm silica-gold core-shell nanoparticles.[103] The dye molecules were tethered to the nanoparticles' surface using a linker containing alkanethiol and oxabicycloheptene moieties. Pulsed laser irradiation of the nanoparticles led to the photothermolysis of the oxabicycloheptene motif *via* a retro Diels-Alder reaction when the temperature was raised to about 60 °C. The heating was confined to the surfaces of the nanoparticles without measurably increasing the temperature of the surroundings; photo-release of fluorescein in live oocytes and tissue cell cultures was demonstrated without killing the cells.

Several other investigators have shown that the conventional photothermal effect can modify the tumour microenvironment. For instance, increased blood flow to the tumour, causing vascular dilation that augmented the enhanced penetration and retention effect (passive targeting), can cause the cell to over express heat shock proteins (HSPs) such as glucose-regulated protein-78 (GRP78).[82,104] These changes could then be exploited for specific targeting of the drug using antibodies or peptides, and to increase vascular permeability and uptake of drugs. Lee *et al*. have developed poly(DL-lactic-co-glycolic acid) gold half-shell nanoparticles loaded with the drug methotrexate for use in rheumatoid arthritis treatment.[105] The drug carrier was conjugated with arginine-glycine-aspartic acid peptides that act as the targeting moiety for inflammation. When exposed to near-infrared irradiation, generation of heat that is due to the photothermal effect caused the drug to be released. Testing in mice found the dual treatment enabled by these nanoparticles has better efficacy than standard methotrexate treatment, which the author attributed to release at above the therapeutic dose. They also showed that higher therapeutic efficacy could be obtained when the chemo-photothermal treatment was combined with

targeted delivery. Similarly, You *et al.*[106] conjugated cyclic peptide c(TNYL-RAW), a second-generation Eph-binding antagonist with improved plasma stability and high-receptor binding affinity, to doxorubicin loaded hollow gold nanoparticles. They showed that the particles were selectively targeted to EphB4-positive tumours, and that concerted chemo-photothermal therapy mediated by the particles resulted in remarkable antitumor efficacy with reduced systemic toxicity, both *in vivo* and *in vitro*.

2.1.3 Other related developments. A key to understanding the drug release mechanisms in photothermal drug release, as well as the implications of *in vivo* use of these nanoparticles, is understanding how the surface temperature of the heated particles vary with particle and laser properties. Bendix *et al*. traps gold nanoparticles in a lipid bilayer which contains a fluorescent dye; the melted footprint around the nanoparticle was used to determine the temperatures reached during laser irradiation.[107] Bendix *et al*. showed that both particle size and laser power were important in determining the temperatures reached during irradiation (See Fig. 6). Kyrsting *et al*. similarly explored the heating profile of gold nanoparticles by placing them in the vicinity of lipid vesicles with temperature sensitive permeability.[108] They found that gold nanoparticles could be heated by several hundred degrees Celsius using laser irradiation. Honda *et al*. monitored the heating of 40 nm gold nanoparticles coated with a thermoresponsive polymer in response to laser light irradiation.[109] The plasmon peak shift that arose from changes in the refractive index of the polymer in response to temperature was monitored. Temperature increases of around 10 °C were noted when the nanoparticles were irradiated with a 1 mW laser at 532 nm.

3 Magnetic hyperthermia induced drug release

Conventional magnetic hyperthermia is a form of cancer therapy that relies on the use of an alternating magnetic field and magnetic nanomaterial to generate heat that induces apoptosis in cancerous tissue.[7] Recently, Kumar and Mohammad suggested broadening the definition of 'hyperthermia' to include magnetically modulated controllable drug delivery.[110] In this context, the heat generated by magnetic hyperthermia is used to induce a change in the therapeutic drug directly, or an agent such as a thermo-responsive polymer or liposome that is conjugated to the drug, resulting in the release of the drug.[111] There is also the possibility of combining both effects of hyperthermia, *i.e*. thermal ablation and drug delivery, as it provides the possibility of further maximising the treatment efficacy. In addition to providing a means for localised heat generation, magnetic nanomaterials have also proven to be beneficial for drug uptake by cancerous cells. The magnetic nanoparticles can be directed and concentrated in the region of interest using a magnet. Moreover, significant increase in cellular uptake of doxorubicin (a model cancer drug) has been demonstrated *in vitro*, when the drug was adsorbed onto tetraheptylammonium capped magnetite and nickel nanoparticles, as compared to standard drug administration.[112] This was attributed to interactions between the magnetic nanoparticles and the drug resistant protein, which in turn reduces the reflux of the doxorubicin, that is, the adsorption of doxorubicin onto the

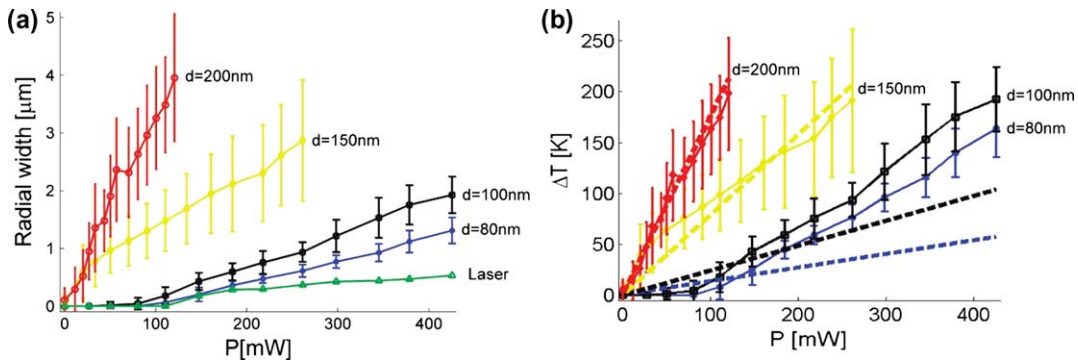

Fig. 6 Bendix *et al.*[107] measurements of surface temperatures of gold nanoparticles. (a) Melted bilayer diameter against laser power: top grey (red online): d = 200 nm; light grey (yellow online): d = 150 nm; black: d = 100 nm; dark grey (blue online): d = 80 nm; bottom grey (green online): laser alone); (b) Temperature of the surface of the gold nanoparticles against laser power (dashed lines given temperature increases as per Mie calculation). Reprinted with permission from P. M. Bendix, S. N. S. Reihani and L. B. Oddershede, *ACS Nano*, 2010, **4**, 2256–2262. Copyright (2010) American Chemical Society.

magnetic nanoparticle surface prevents it from being pumped out of the cell by the drug resistant protein.[58]

3.1 Recent developments in the application of nanomaterials for magnetic hyperthermia induced drug release

3.1.1 Design and synthesis of nanomaterials for magnetic hyperthermia applications. A number of materials can be used as magnetic responsive nanoparticles in magnetic hyperthermia induced drug release. The majority of studies focus on the use of iron oxide, primarily magnetite (Fe_3O_4) and maghemite (γ-Fe_2O_3). This is due to their well-understood and facile synthesis methods, as well as the relative ease with which biocompatibility can be achieved. The method of choice for producing magnetite is the co-precipitation of Fe^{2+} and Fe^{3+} at elevated temperatures (70–100 °C) in the presence of a base.[113] The magnetite particles can be oxidised to maghemite by peptizing in nitric acid. It is a challenge to obtain tailored morphologies (*i.e.* non-spheroid) and/or particles with high magnetisation using contemporary co-precipitation methods. Alternative synthesis methodologies for magnetite nanoparticles have thus been developed; these include co-precipitation of Fe^{2+} and Fe^{3+} in the presence of sodium carbonate,[114] forced hydrolysis of iron (II) hydroxide in a nitrogen atmosphere,[115] electro-oxidation in the presence of a stabilising surfactant,[116] and hydrogen reduction of other iron oxide crystals (*e.g.* hematite)[117] at elevated temperatures.

The use of metallic nanomaterials for magnetic hyperthermia has also attracted much interest recently due to their superior magnetic properties and ease of manipulating the size and morphology, when compared to iron oxide based nanoparticles.[118] Some recent developments in this area include the synthesis of Fe-Pt, Fe-Pd and Fe-Pt-Pd alloys with a range of shapes and sizes.[119] Lu *et al.* outlined the synthesis of magnetic cobalt nanomaterials by the reduction of Co^{2+} in the presence of a polymer ligand.[120] It is important to note that the chemical composition of many magnetic alloys renders them inherently toxic.[121] For these nanomaterials to be accepted as feasible drug carriers, the toxicity issues must be addressed. Other related developments include the use of laser ablation of iron foil to synthesise superparamagnetic Fe_3C,[122] and the synthesis of $MnFe_2O_4$ and $Mn_{1-x}Zn_xFe_2O_4$ by wet chemical co-precipitation,[45,123] and the synthesis of mesoporous $MgFe_2O_3$ from the reduction of iron (III) chloride[124] in the presence of magnesium chloride.

Investigations were also directed towards increasing the drug loading capacity of magnetic nanoparticles. Chen *et al.* synthesised magnetic silica nanotubes by first depositing hematite (α-Fe_2O_3), followed by silica, onto a carbon nanotube template.[11] The carbon template was removed and the hematite reduced to magnetite by heating the nanoparticles to 800 °C under argon. The magnetite was then oxidized to maghemite (γ-Fe_2O_3) by heating at 600 °C. Chen *et al.* claimed the open-ended tubular structure renders the magnetic silica tubes potentially applicable in hyperthermia induced drug delivery, particularly of high molecular weight therapeutic agents such as DNA or RNA.

Nanocarriers that respond to more than one stimulus have also been developed. Sahoo *et al*. developed a dual pH and temperature responsive system by tethering magnetite nanoparticles with poly(N-ispropylacrylamide)-block-poly(acrylic acid) copolymers.[48] Doxorubicin was electrostatically attached to the negatively charged poly(acrylic acid) segment of the polymer chain. The pH-responsive drug release was attributed to protonation of the carboxylic groups on the polymer chain, resulting in weaker drug-polymer interactions. The temperature-responsive nature of the agent was conferred by the thermo-responsive PNIPAM polymer block (LCST = 31 °C). The cytotoxicity, uptake and therapeutic effects of the nanocarrier was demonstrated *in vitro*, although magnetic hyperthermia induced release of the drug was not demonstrated. By combining the pH and temperature stimuli, it was found that drug release rate could be significantly increased from approximately 11% at pH 7.4 and 25 °C, to 75% at pH 5.0 and 37 °C after a period of 5 h.

Bilalis *et al*. fabricated polymeric 'microcontainers' that responded to pH, redox and magnetic induction.[125] As outlined in Fig. 7, these 'microcontainers' were synthesised by a two-stage distillation precipitation polymerisation procedure followed by sacrificial core dissolution, resulting in a poly(methacrylic acid) shell with disulfide (S–S) bonds ($PMAA_{S\text{-}S}$). These microcontainers were then decorated with magnetic nanoparticles and loaded with daunorubicin hydrochloride (a model drug). Bilalis *et al*. showed increased release of the drug from 15% to 40% when pH was

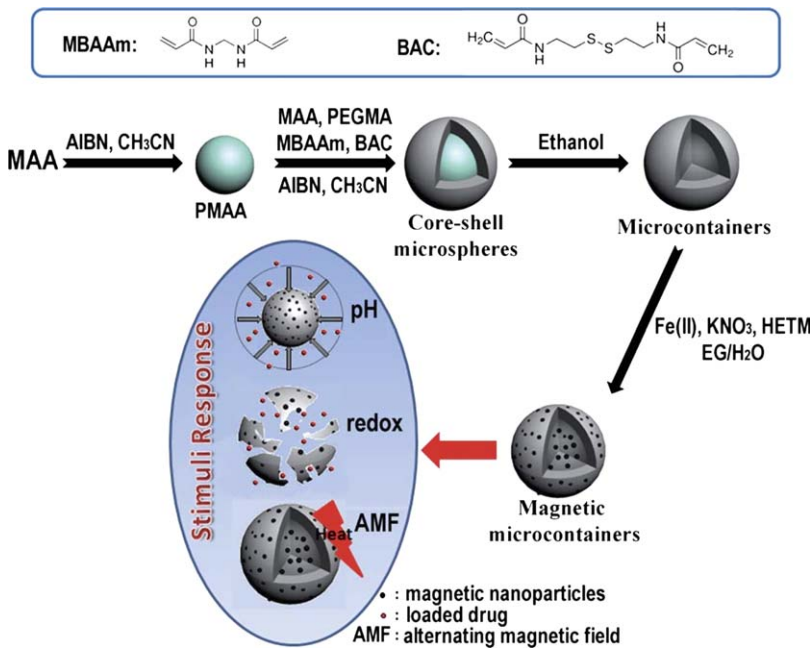

Fig. 7 Schematic illustration of the synthesis procedure for the preparation of magnetic microcontainers. Chemical structures of crosslinkers are also illustrated.[125] Reproduced from P. Bilalis, A. Chatzipavlidis, L.-A. Tziveleka, N. Boukos and G. Kordas, *Journal of Materials Chemistry*, 2012, **22**, 13451–13454 with permission from The Royal Society of Chemistry.

decreased from 5 to 7.4, and to 94% when glutathione concentration was increased from 0 to 20 mM. They further showed that the microcontainers can be used to generate heat in an alternating magnetic field, but did not demonstrate magnetic hyperthermia induced drug release for their microcontainers.

3.1.2 Magnetic hyperthermia induced controllable drug release. Kumar *et al.* prepared polyethylene glycol coated, carboxyl-enriched, mesoporous $MgFe_2O_4$ by a polyol method.[46] They showed that an 80% loading efficiency of doxorubicin could be achieved due to the highly negative surface charge and mesoporous nature of the particles. Magnetic hyperthermia in combination with drug therapy was shown to lead to the death of approximately 90% of cells *in vitro*, as compared to 40–45% cell death when only magnetic hyperthermia was applied. It is important to note here that polyethylene glycol confers size stability and biocompatibility properties to the particles, but it is not expected to play a role in the heat induced release of the drug in this work. Instead, pH enhanced release of doxorubicin was observed in a mild acidic environment; this was attributed to the dissolution of the polyethylene glycol and weakening of electrostatic bonding by excessive deprotonation of the daunosamine group of the doxorubicin molecule.

Sivakumar *et al.* incorporated superparamagnetic fluorescent nanoparticles and 5-fluorouracil (a chemotherapeutic anticancer drug) into a biopolymer matrix formed by carboxymethyl cellulose, a water-soluble cellulose with carboxymethyl groups bonded to some of the hydroxyl groups on the cellulose backbone.[126] Folate conjugated to the carboxymethyl cellulose backbone enabled the drug carrier to be targeted to folate-receptor tumour markers that are over expressed in cancer cells. Similarly, Brulé *et al.* and Arias *et al.* incorporated maghemite cores into alginate and polyalkylcyanoacrylates matrices, respectively.[127,128] In the work of Arias *et al.*, the presence of the polyalkylcyanoacrylates matrix was shown to increase the amount of drugs loaded, with both the drug loading and entrapment efficiency increasing with increased drug concentration during the loading step. The amount of methotrexate that is loaded can also be increased by introducing a surfactant (Pluronic® F-68) and by increasing the rate of polymerisation; nonetheless, a polymerisation rate that is too rapid can produce undesirable precipitates. Sivakumar *et al.* and Arias *et al.* did not explicitly study the hyperthermia induced drug release properties of the drug carrier. Nonetheless, Sivakumar *et al.* did show that combined treatment of cancer cells with the drug and magnetic hyperthermia synergistically killed almost 95% of cancer cells. Brulé *et al.* showed hyperthermia significantly enhanced the effect of doxorubicin, with MCF-7 cells exhibiting viable cell coverage of $5.7\% \pm 4.2\%$ when exposed to the combined therapy, as opposed to $>50\%$ when treated with only doxorubicin-loaded microbeads or application of hyperthermia.

Mi *et al.* co-encapsulated magnetite nanoparticles and docetaxel (a model anticancer agent) within a matrix consisting of mixed copolymers of poly(lactide)-D-alpha-tocopheryl polyethylene glycol succinate and carboxyl group terminated tocopheryl polyethylene glycol succinate.[129] The carboxyl group terminated tocopheryl polyethylene glycol succinate

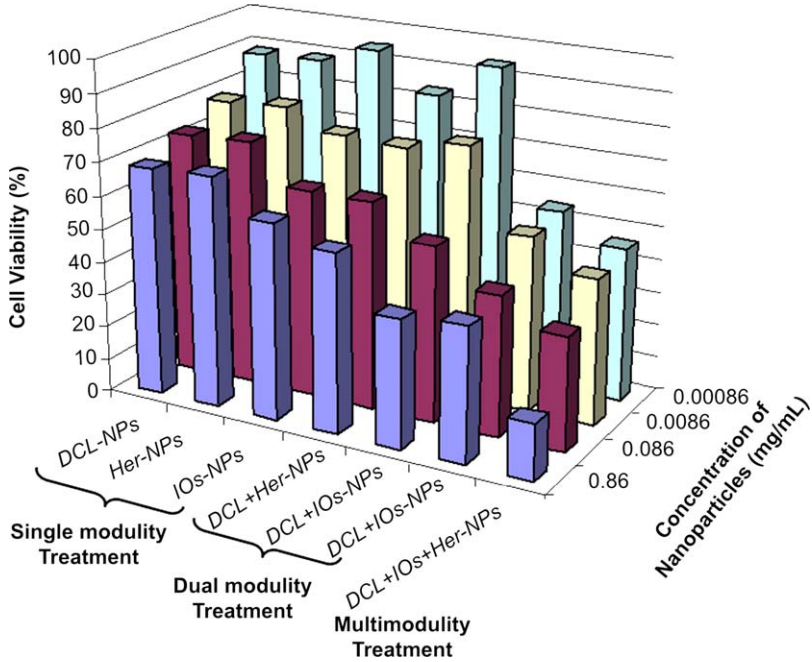

Fig. 8 Analysis of SK-BR-3 cell viability as a result of exposure to multimodal treatment herception vonjugated, thermomagnetic iron oxides and docetaxel loaded nanoparticles after 24 h incubation and 12 h recovery.[129] Reprinted from Y. Mi, X. Liu, J. Zhao, J. Ding and S.-S. Feng, Multimodality treatment of cancer with herceptin conjugated, thermomagnetic iron oxides and docetaxel loaded nanoparticles of biodegradable polymers Biomaterials, *Biomaterials*, **33**, 7519–7529, Copyright (2012), with Permission from Elsevier.

enabled herceptin to be conjugated *via* carbodiimide chemistry for biotherapy and cell targeting; the polymer was also purported to have anti-cancer and neuroprotective properties. Using this platform, Mi *et al.* demonstrated that multimodal treatment of cancer (where cell-targeting, chemotherapy, hyperthermic therapy and biological therapy are combined) shows superior *in vitro* therapeutic efficacy than single modality or dual modality treatment under all the nanoparticle concentrations tested (see Fig. 8).[129]

Recent studies have also examined the use of PNIPAM in dual responsive drug delivery systems; that is, the drug is released in response to more than one stimulus, most commonly temperature and pH. This would be highly advantageous as it would potentially improve the accuracy and control of the drug delivery mechanism. Chiang *et al.* developed superparamagnetic iron oxide nanoparticles loaded hybrid nanogels for both pH and temperature responsive delivery of doxorubicin.[130] The hybrid nanogels were co-assembled with acrylic acid/2-methacryloylethyl acrylate/ $mPEG_{2000}$/$PNIPA_{3000}$ copolymer SPIONs. Over 24 h at 37 °C, 17% release was observed at pH 7.4, and 55% release at pH 5.0. Release rates were notably increased through exposure to an alternating magnetic field.

Other recent studies have investigated the integration of nanoparticles into polymersomes to yield heat responsive drug delivery agents. Sanson *et al.* developed polymeric vesicles (polymersomes) which consist of

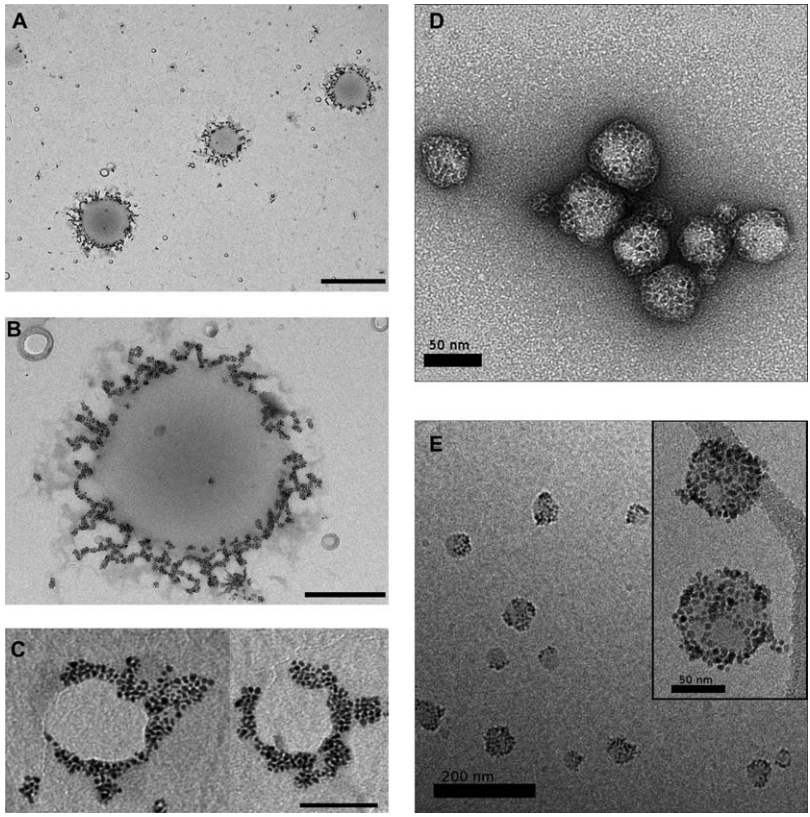

Fig. 9 TEM images of USPIO-loaded vesicles prepared by nanoprecipitation. (A) Low magnification picture of WD15–50 vesicles (scale bar 1 μm). (B) Close-up view of a WD15–50 vesicle containing ~1500 USPIOs as measured by image analysis (scale bar 300 nm). (C) WDi-70 vesicles spreading on the substrate, which enables counting ~190 USPIOs on the left and ~220 USPIOs on the right (scale bar 100 nm). (D) Image of negatively stained WDi-50 vesicles, showing a group of vesicles laying intact on the carbon substrate (scale bar 50 nm). (E) Cryo-TEM image showing homogeneously dispersed WDi-50 vesicles (scale bar 200 nm). (Inset) Close-up view of two vesicles showing a mantle of respectively ~80 and ~110 close-packed USPIOs with some uncovered areas (scale bar 50 nm).[24] Reprinted with permission from C. Sanson, O. Diou, J. Thévenot, E. Ibarboure, A. Soum, A. Brûlet, S. Miraux, E. Thiaudière, S. Tan, A. Brisson, V. Dupuis, O. Sandre and S. Lecommandoux, *ACS Nano*, 2011, **5**, 1122–1140. Copyright (2011) American Chemical Society.

hydrophobically modified maghemite (γ-Fe_2O_3) nanoparticles that were encapsulated within the membrane of poly(trimethylene carbonate)-b-poly(L-glutamic acid) (PTMC-b-PGA) block copolymer vesicles using a nanoprecipitation process (See Fig. 9). In a subsequent study, they showed that when a high frequency alternating magnetic field was applied to the polymersomes loaded with 6% (w/w) of doxorubicin and 30% (w/w) of superparamagnetic iron oxide nanoparticles, an 18% increase in cell toxicity was observed for HeLa cells that had internalised the polymersome.[24,131] Moreover, they were able to show that the cytotoxicity effects arose from the increased doxorubicin release and not from a pure magnetic hyperthermia effect. That is, when polymersomes loaded with magnetic nanoparticles only were tested, no cytotoxicity effect was observed. Their results

indicate that the applied magnetic field induces a localised hyperthermia effect that leads to increased drug release, but not cell death as would have occurred in conventional hyperthermia treatment.

Hu *et al.* prepared core-shell, double-emulsion multi-drug carriers in a facile one step emulsifying process where poly(vinyl alcohol) and magnetic iron oxide nanoparticles are use as surfactants and stabilisers, respectively.[132] They were able to incorporate a hydrophilic drug (doxorubicin) into the core and a hydrophobic drug (paclitaxel) into the shell of the emulsion, and release them upon the application of an alternating magnetic field. The hydrophilic-lipophilic balance value of poly(vinyl alcohol) was shown to be an important factor in determining the construct of the emulsion, with intermediate molecular weight poly(vinyl alcohol) (47 kDa) favouring the formation of water-in-oil-in-water (W/O/W) double emulsion. Moreover, the inclusion of iron oxide nanoparticles was shown to be critical to the formation of a stable and robust W/O/W emulsion. The magnetic hyperthermia induced drug release was also shown to be dependent on the molecular weight of poly(vinyl alcohol), with faster drug release observed for lower molecular weight polymers due to the differences in the chain flexibility and mobility. It was observed that the initial release of doxorubicin was slower than that of paclitaxel; this was explained by the more rapid heating of the magnetic iron oxide nanoparticles impregnated within the hydrophobic shell in which the paclitaxel resided. As the temperature rose then spread to the emulsion core, a faster release of doxorubicin, further aided by its affinity to water, was realized. Using a peptide (IVO24) as the targeting agent, Hu *et al.* demonstrated that the double emulsions have good biocompatibility and can achieve better treatment efficacy both *in vivo* and *in vitro*.

3.1.3 Other related developments. One of the major issues faced by researchers in the field of magnetic induction hyperthermia is measurement of the temperature profile and heat released by the nanocomposite in response to an alternating magnetic field. This information would assist in the design and refinement of the nanoparticle-polymer systems in order to achieve more efficient release mechanisms. Recently, however, Riedinger *et al.* have developed a clever solution to this problem. Fluoresceinamine (a doxorubicin substitute) was bound to an azobis[N-(2-carboxyethyl)-2-methylpropionamidine] molecule which was in turn bonded to a polyethylene glycol spacer molecules (differing in length) on the surface of magnetite nanoparticles.[44] By varying the lengths of the PEG spacers, they were able to hold the drug at varying distances from the surface of the nanoparticle. By measuring whether the drug was release when the nanoparticles were heated up by magnetic induction, they could determine whether the heat of the nanoparticle was sufficient to break the azo bond. Whilst this agent could feasibly be used for drug delivery, the primary purpose of this study was to conduct sub-nanometer temperature probing.

4 Concluding remarks

Recent studies on the use of nanomaterial mediated photothermal and magnetic hyperthermia induced drug release highlight the potential of these

platforms for cancer therapy. Potent drugs are sequestered within a nanocarrier until it is delivered to the site of diseased tissue, where it is released in a time and site-specific manner in response to heat generated by the photothermal or magnetic hyperthermia effects. The benefits of these controllable drug delivery platforms are numerous. Chiefly, drug dosage can be increased without amplifying the negative side effects of chemotherapy leading to an improvement in the treatment efficacy. The *in vitro* and *in vivo* studies outlined herein further showed that composites of polymer and plasmonic or magnetic nanomaterials are ideal drug carriers for these platforms. Inorganic nanomaterials such as gold and magnetite act as heat generators in response to the light or alternating magnetic field stimuli, while the polymer provides a drug storage/release mechanism and improves the *in vivo* stability and biocompatibility of the drug carrier.

Before photothermal and magnetic hyperthermia induced drug delivery can proceed to clinical trials and applications, some questions and limitations have to be addressed. It would be of interest to see to what extent dosage and drug delivery can be fine-tuned by using these platforms. The delivery of a wider range of drugs, and stability of these drugs when exposed to heat should also be considered. Issues with low drug loading capacity and premature release of the drug from the carrier must also be addressed; the former by selecting nanostructures with high drug loading capacity, and the latter *via* strategies such as polymersomes with improved structural integrity or heat labile bonds to chemically bind the drug to the carrier.[82,83,133] Studies in cultured cells and mice models have been promising, nonetheless, large animal studies are still required to confirm the platforms' biocompatibility, biodistribution, uptake into diseased cells and overall efficacy. Issues related to the application of light and alternating magnetic fields in a clinical setting should also be considered. For instance, the use of fiber-optic micro-needles to deliver light directly to deeper tissue has been proposed.[134]

The mechanism behind the increased efficacy is also not fully elucidated in some studies. For instance, it is not always clear if the increased efficacy is due to the action of the drug alone, or the photothermal or magnetic hyperthermia heating has induced physiological change to the diseased tissue, thereby increasing the uptake of the drug. Recent advancement in cellular biology and drug carriers can also expand the opportunities and methodologies to be considered in photothermal and magnetic hyperthermia induced drug delivery. Newly identified endothelial cell surface receptors and the release of heat shock proteins when cells are exposed to heat can be used to improved recognition and targeting of diseased cells. Thermoresponsive polypeptide drug-conjugates raise the potential for pH responsive drug delivery, and if gold or magnetic nanoparticles can be incorporated into the design, there would be potential for pH-temperature dual responsive drug delivery.[135–137]

The combination of photothermal and magnetic hyperthermia drug delivery with biomedical imaging, in a parallel area of research called 'theranostics', is also of interest. The metallic and magnetic nanoparticles used in the design of the drug carriers also have potential application as contrast agents in medical imaging. Notably, magnetic iron oxide nanoparticles have been shown to improve the image obtained in magnetic

resonance imaging.[138] Laboratory studies have also shown gold and silica to be ideal contrast agents in X-ray computed tomography,[139] photo-acoustic[140] and ultrasound imaging.[141] With the ability to correlate imaging with drug therapy, the effects of each component of the drug carrier (materials selection and design, targeting, drug loading) on each step in the delivery cascade may be assessed and quantified in an absolute manner; this should lead to a better understanding of how drug design and administration protocol affects the pharmacokinetics of the drug carrier, as well as the treatment efficacy.

References

1 Y. Ma, X. Liang, S. Tong, G. Bao, Q. Ren and Z. Dai, *Advanced Functional Materials*, 2013, **23**, 815–822.
2 S. Ramishetti and L. Huang, *Therapeutic Delivery*, 2012, **3**, 1429–1445.
3 Y. Shao, W. Huang, C. Shi, S. T. Atkinson and J. Luo, *Therapeutic Delivery*, 2012, **3**, 1409–1427.
4 O. C. Steinbach, *Therapeutic Delivery*, 2012, **3**, 1373–1377.
5 R. Petros and J. DeSimone, *Nature Reviews*, 2010, **9**, 615–627.
6 R. K. Jain, *Nat Med.*, 2001, **7**, 987–989.
7 D. Ortega and Q. A. Pankhurst, In *Nanoscience: Volume 1: Nanostructures through Chemistry*, The Royal Society of Chemistry, Cambridge, 2013, vol. 1, pp. 60–88.
8 A. O. Govorov and H. H. Richardson, *Nano Today*, 2007, **2**, 30–38.
9 S.-H. Wu, C.-Y. Mou and H.-P. Lin, *Chem. Soc. Rev.*, 2013, **42**, 3862–3875.
10 P.-J. Chen, S.-H. Hu, C.-S. Hsiao, Y.-Y. Chen, D.-M. Liu and S.-Y. Chen, *J. Mat. Chem.*, 2011, **21**, 2535–2543.
11 X. Chen, R. Klingeler, M. Kath, A. A. El Gendy, K. Cendrowski, R. J. Kalenczuk and E. Borowiak-Palen, *ACS Applied Materials & Interfaces*, 2012, **4**, 2303–2309.
12 J. Jaber and E. Mohsen, *Colloids and Surfaces B: Biointerfaces*, 2013, **102**, 265–272.
13 J. Liu, S. Z. Qiao, S. Budi Hartono and G. Q. Lu, *Angewandte Chemie International Edition*, 2010, **49**, 4981–4985.
14 Q. Mu, L. Yang, J. C. Davis, R. Vankayala, K. C. Hwang, J. Zhao and B. Yan, *Biomaterials*, 2010, **31**, 5083–5090.
15 Q. Zhang, W. Wang, J. Goebl and Y. Yin, *Nano Today*, 2009, **4**, 494–507.
16 T. Zhang, Q. Zhang, J. Ge, J. Goebl, M. Sun, Y. Yan, Y.-s. Liu, C. Chang, J. Guo and Y. Yin, *J. Phys. Chem. C*, 2009, **113**, 3168–3175.
17 Y. Zhao and L. Jiang, *Advanced Materials*, 2009, **21**, 3621–3638.
18 T. Zhang, J. Ge, Y. Hu, Q. Zhang, S. Aloni and Y. Yin, *Angewandte Chemie International Edition*, 2008, **47**, 5806–5811.
19 Y. Sun, B. T. Mayers and Y. Xia, *Nano Letters*, 2002, **2**, 481–485.
20 Y. Sun and Y. Xia, *Science*, 2002, **298**, 2176–2179.
21 J. Champion, A. Walker and S. Mitragotri, *Pharm Res.*, 2008, **25**, 1815–1821.
22 H. Zhang, D. Pan, K. Zou, J. He and X. Duan, *J. Mat. Chem.*, 2009, **19**, 3069–3077.
23 H. Ai, *Advanced Drug Delivery Reviews*, 2011, **63**, 772–788.
24 C. Sanson, O. Diou, J. Thévenot, E. Ibarboure, A. Soum, A. Brûlet, S. Miraux, E. Thiaudière, S. Tan, A. Brisson, V. Dupuis, O. Sandre and S. Lecommandoux, *ACS Nano*, 2011, **5**, 1122–1140.
25 H. Oliveira, E. Pérez-Andrés, J. Thevenot, O. Sandre, E. Berra and S. Lecommandoux, *Journal of Controlled Release*, 2013, **169**, 165–170.

26 W. B. Liechty, D. R. Kryscio, B. V. Slaughter and N. A. Peppas, *Annual Review of Chemical and Biomolecular Engineering*, 2010, **1**, 149–173.
27 C. Boyer, M. R. Whittaker, V. Bulmus, J. Liu and T. P. Davis, *NPG Asia Mater*, 2010, **2**, 23–30.
28 O. Pillai and R. Panchagnula, *Current Opinion in Chemical Biology*, 2001, **5**, 447–451.
29 R. B. Grubbs, *Polymer Reviews*, 2007, **47**, 197–215.
30 A. K. Iyer, G. Khaled, J. Fang and H. Maeda, *Drug Discovery Today*, 2006, **11**, 812–818.
31 U. Prabhakar, H. Maeda, R. K. Jain, E. M. Sevick-Muraca, W. Zamboni, O. C. Farokhzad, S. T. Barry, A. Gabizon, P. Grodzinski and D. C. Blakey, *Cancer Research*, 2013, **73**, 2412–2417.
32 K. Greish, *Drug Discovery Today: Technologies*, 2012, **9**, e161–e166.
33 C. Boyer, M. R. Whittaker, M. Luzon and T. P. Davis, *Macromolecules*, 2009, **42**, 6917–6926.
34 R. Gref, M. Luck, P. Quellec, M. Marchand, E. Dellacherie, S. Harnisch, T. Blunk and R. H. Muller, *Colloids Surf., B Biointerfaces*, 2000, **18**, 301–313.
35 C. Flesch, Y. Unterfinger, E. Bourgeat-Lami, E. Duguet, C. Delaite and P. Dumas, *Macromol. Rapid Commun.*, 2005, **26**, 1494–1498.
36 S. Laurent, D. Forge, M. Port, A. Roch, C. Robic, L. Vander Elst and R. N. Muller, *Chemical Reviews*, 2008, **108**, 2064–2110.
37 I. Banerjee, R. C. Pangule and R. S. Kane, *Advanced Materials*, 2011, **23**, 690–718.
38 P. Aggarwala, J. B. Halla, C. B. McLelanda, M. A. Dobrovolskaia and S. E. McNeil, *Advanced Drug Delivery Reviews*, 2009, **61**, 428–437.
39 G. Prencipe, S. M. Tabakman, K. Welsher, Z. Liu, A. P. Goodwin, L. Zhang, J. Henry and H. Dai, *J. Am. Chem. Soc.*, 2009, **131**, 4783–4787.
40 C. Boyer, V. Bulmus, T. P. Davis, V. Ladmiral, J. Liu and S. b. Perrier, *Chemical Reviews*, 2009, **109**, 5402–5436.
41 J. S. Basuki, L. Esser, P. B. Zetterlund, M. R. Whittaker, C. Boyer and T. P. Davis, *Macromolecules*, 2013, **46**, 6038–6047.
42 R. Tedja, A. H. Soeriyadi, M. R. Whittaker, M. Lim, C. Marquis, C. Boyer, T. P. Davis and R. Amal, *Polymer Chemistry*, 2012, **3**, 2743–2751.
43 W. Wu, J. Shen, Z. Gai, K. Hong, P. Banerjee and S. Zhou, *Biomaterials*, 2011, **32**, 9876–9887.
44 A. Riedinger, P. Guardia, A. Curcio, M. A. Garcia, R. Cingolani, L. Manna and T. Pellegrino, *Nano Letters*, 2013, **13**, 2399–2406.
45 S. A. Shah, M. H. Asdi, M. U. Hashmi, M. F. Umar and S.-U. Awan, *Materials Chemistry and Physics*, 2012, **137**, 365–371.
46 S. Kumar, A. Daverey, N. K. Sahu and D. Bahadur, *J. Mat. Chem. B*, 2013, **1**, 3652–3660.
47 L. Jianbo, Q. Yang, R. Jie, Y. Weizhong and S. Donglu, *Nanotechnology*, 2012, **23**, 505706.
48 B. Sahoo, K. S. P. Devi, R. Banerjee, T. K. Maiti, P. Pramanik and D. Dhara, *ACS Applied Materials & Interfaces*, 2013, **5**, 3884–3893.
49 C. Weber, R. Hoogenboom and U. S. Schubert, *Progress in Polymer Science*, 2012, **37**, 686–714.
50 R. Cheng, F. Meng, C. Deng, H.-A. Klok and Z. Zhong, *Biomaterials*, 2013, **34**, 3647–3657.
51 S. R. Deka, A. Quarta, R. Di Corato, A. Riedinger, R. Cingolani and T. Pellegrino, *Nanoscale*, 2011, **3**, 619–629.
52 H. G. Schild, *Progress in Polymer Science*, 1992, **17**, 163–249.
53 A. Yao, Q. Chen, F. Ai, D. Wang and W. Huang, *J. Mater. Sci.: Mater Med.*, 2011, **22**, 2239–2247.

54 M. I. Shukoor, F. Natalio, H. A. Therese, M. N. Tahir, V. Ksenofontov, M. Panthfer, M. Eberhardt, P. Theato, H. C. Schrder, W. E. G. Mller and W. Tremel, *Chem. Mater.*, 2008, **20**, 3567–3573.
55 F. Zhang and C.-C. Wang, *Langmuir*, 2009, **25**, 8255–8262.
56 H. Lee, E. Lee, D. K. Kim, N. K. Jang, Y. Y. Jeong and S. Jon, *J. Am. Chem. Soc.*, 2006, **128**, 7383–7389.
57 R. Narain, M. Gonzales, A. S. Hoffman, P. S. Stayton and K. M. Krishnan, *Langmuir*, 2007, **23**, 6299–6304.
58 G. Huang, C. Zhang, S. Li, C. Khemtong, S.-G. Yang, R. Tian, J. D. Minna, K. C. Brown and J. Gao, *J. Mat. Chem.*, 2009, **19**, 6367–6372.
59 E. Amstad, S. Zurcher, A. Mashaghi, J. Y. Wong, M. Textor and E. Reimhult, *Small*, 2009, **5**, 1334–1342.
60 X. He, X. Wu, X. Cai, S. Lin, M. Xie, X. Zhu and D. Yan, *Langmuir*, 2012, **28**, 11929–11938.
61 R. D. Palma, S. Peeters, M. J. V. Bael, H. V. d. Rul, K. Bonroy, W. Laureyn, J. Mullens, G. Borghs and G. Maes, *Chem. Mater.*, 2007, **19**, 1821–1831.
62 S. Slavin and D. M. Haddleton, *Soft Matter*, 2012, **8**, 10388–10393.
63 S. Slavin, A. H. Soeriyadi, L. Voorhaar, M. R. Whittaker, C. R. Becer, C. Boyer, T. P. Davis and D. M. Haddleton, *Soft Matter*, 2012, **8**, 118–128.
64 Y.-C. Yeh, B. Creran and V. M. Rotello, *Nanoscale*, 2012, **4**, 1871–1880.
65 C. Boyer, M. H. Stenzel and T. P. Davis, *J. Polymer Science Part A: Polymer Chemistry*, 2011, **49**, 551–595.
66 K. Matyjaszewski, *Macromolecules*, 2012, **45**, 4015–4039.
67 N. H. Nguyen, M. E. Levere and V. Percec, *J. of Polymer Science Part A: Polymer Chemistry*, 2012, **50**, 860–873.
68 J. Nicolas, Y. Guillaneuf, C. Lefay, D. Bertin, D. Gigmes and B. Charleux, *Progress in Polymer Science*, 2013, **38**, 63–235.
69 K. Matyjaszewski and J. Spanswick, *Materials Today*, 2005, **8**, 26–33.
70 S. Hansson, V. Trouillet, T. Tischer, A. S. Goldmann, A. Carlmark, C. Barner-Kowollik and E. Malmström, *Biomacromolecules*, 2012, **14**, 64–74.
71 M. Lattuada and T. A. Hatton, *Langmuir*, 2007, **23**, 2158–2168.
72 J. Tian, Y. K. Feng and Y. S. Xu, *Macromol. Res.*, 2006, **14**, 209–213.
73 L. Wang, K. G. Neoh, E. T. Kang, B. Shuter and S.-C. Wang, *Advanced Functional Materials*, 2009, **19**, 2615–2622.
74 J. E. Moses and A. D. Moorhouse, *Chem. Soc. Rev.*, 2007, **36**, 1249 –1262.
75 C. D. Hein, X.-M. Liu and D. Wang, *Pharm. Res.*, 2008, **25**, 2216–2230.
76 M. A. White, J. A. Johnson, J. T. Koberstein and N. J. Turro, *J. Am. Chem. Soc.*, 2006, **128**, 11356–11357.
77 L. Castaneda, A. Maruani, F. F. Schumacher, E. Miranda, V. Chudasama, K. A. Chester, J. R. Baker, M. E. B. Smith and S. Caddick, *Chem. Comm.*, 2013, **49**, 8187–8189.
78 S. R. MacEwan, D. J. Callahan and A. Chilkoti, *Nanomedicine*, 2010, **5**, 793–806.
79 J. Liu, H. Duong, M. R. Whittaker, T. P. Davis and C. Boyer, *Macromolecular Rapid Communications*, 2012, **33**, 760–766.
80 S. Yamashita, H. Fukushima, Y. Akiyama, Y. Niidome, T. Mori, Y. Katayama and T. Niidome, *Bioorganic & Medicinal Chemistry*, 2011, **19**, 2130–2135.
81 Z. Erno, A. M. Asadirad, V. Lemieux and N. R. Branda, *Organic & Biomolecular Chemistry*, 2012, **10**, 2787–2792.
82 M. P. Melancon, A. M. Elliott, A. Shetty, Q. Huang, R. J. Stafford and C. Li, *Journal of Controlled Release*, 2011, **156**, 265–272.
83 S. Vijayakumar and S. Paulsi, *International Journal of Pharmaceutical Sciences Review and Research*, 2013, **20**, 80–88.

84 A. M. Alkilany, L. B. Thompson, S. P. Boulos, P. N. Sisco and C. J. Murphy, *Advanced Drug Delivery Reviews*, 2012, **64**, 190–199.
85 A. Mandelis, *Opt. Photon. News*, 2002, **13**, 32–37.
86 A. Mandelis and Y. Riopel, *Journal of Vacuum Science & Technology A*, 2000, **18**, 705–708.
87 J. Robinson, K. Welsher, S. Tabakman, S. Sherlock, H. Wang, R. Luong and H. Dai, *Nano Res*, 2010, **3**, 779–793.
88 J. Lin, S. Wang, P. Huang, Z. Wang, S. Chen, G. Niu, W. Li, J. He, D. Cui, G. Lu, X. Chen and Z. Nie, *ACS Nano*, 2013, **7**, 5320–5329.
89 M. Zheng, C. Yue, Y. Ma, P. Gong, P. Zhao, C. Zheng, Z. Sheng, P. Zhang, Z. Wang and L. Cai, *ACS Nano*, 2013, **7**, 2056–2067.
90 J. Huang, K. S. Jackson and C. J. Murphy, *Nano Letters*, 2012, **12**, 2982–2987.
91 D. Liu, X. Wang, S. Han and X. Zhao, *Gaofenzi Cailiao Kexue Yu Gongcheng*, 2011, **27**, 172–175.
92 Z. Fan, D. Senapati, A. K. Singh and P. C. Ray, *Molecular Pharmaceutics*, 2012, **10**, 857–866.
93 J. Li, J. Han, T. Xu, C. Guo, X. Bu, H. Zhang, L. Wang, H. Sun and B. Yang, *Langmuir*, 2013, **29**, 7102–7110.
94 H. Zhang, C. Chen, L. Hou, N. Jin, J. Shi, Z. Wang, Y. Liu, Q. Feng and Z. Zhang, *Journal of Drug Targeting*, 2013, **21**, 312–319.
95 M. J. O'Connell, S. M. Bachilo, C. B. Huffman, V. C. Moore, M. S. Strano, E. H. Haroz, K. L. Rialon, P. J. Boul, W. H. Noon, C. Kittrell, J. Ma, R. H. Hauge, R. B. Weisman and R. E. Smalley, *Science*, 2002, **297**, 593–596.
96 A. C. Estrada, A. L. Daniel-da-Silva and T. Trindade, *RSC Advances*, 2013, **3**, 10828–10836.
97 A. Sahu, W. I. Choi, J. H. Lee and G. Tae, *Biomaterials*, 2013, **34**, 6239–6248.
98 Y. Wang, K. Wang, J. Zhao, X. Liu, J. Bu, X. Yan and R. Huang, *Journal of the American Chemical Society*, 2013, **135**, 4799–4804.
99 H. Liu, D. Chen, L. Li, T. Liu, L. Tan, X. Wu and F. Tang, *Angewandte Chemie International Edition*, 2011, **50**, 891–895.
100 Z. Jiang, B. Dong, B. Chen, J. Wang, L. Xu, S. Zhang and H. Song, *Small*, 2013, **9**, 604–612.
101 G. D. Moon, S.-W. Choi, X. Cai, W. Li, E. C. Cho, U. Jeong, L. V. Wang and Y. Xia, *Journal of the American Chemical Society*, 2011, **133**, 4762–4765.
102 S. Yamashita, H. Fukushima, Y. Niidome, T. Mori, Y. Katayama and T. Niidome, *Langmuir*, 2011, **27**, 14621–14626.
103 W. F. Zandberg, A. B. S. Bakhtiari, Z. Erno, D. Hsiao, B. D. Gates, T. Claydon and N. R. Branda, *Nanomedicine: Nanotechnology, Biology and Medicine*, 2012, **8**, 908–915.
104 A. J. Gormley, N. Larson, S. Sadekar, R. Robinson, A. Ray and H. Ghandehari, *Nano today*, 2012, **7**, 158–167.
105 S.-M. Lee, H. J. Kim, Y.-J. Ha, Y. N. Park, S.-K. Lee, Y.-B. Park and K.-H. Yoo, *ACS Nano*, 2012, **7**, 50–57.
106 J. You, R. Zhang, C. Xiong, M. Zhong, M. Melancon, S. Gupta, A. M. Nick, A. K. Sood and C. Li, *Cancer Research*, 2012, **72**, 4777–4786.
107 P. M. Bendix, S. N. S. Reihani and L. B. Oddershede, *ACS Nano*, 2010, **4**, 2256–2262.
108 A. Kyrsting, P. M. Bendix, D. G. Stamou and L. B. Oddershede, *Nano Letters*, 2010, **11**, 888–892.
109 M. Honda, Y. Saito, N. I. Smith, K. Fujita and S. Kawata, *Opt. Express*, 2011, **19**, 12375–12383.
110 C. S. S. R. Kumar and F. Mohammad, *Advanced Drug Delivery Reviews*, 2011, **63**, 789–808.

111 J. Zhang and R. D. K. Misra, *Acta Biomaterialia*, 2007, **3**, 838–850.
112 R. Zhang, C. Wu, X. Wang, Q. Sun, B. Chen, X. Li, S. Gutmann and G. Lv, *Materials Science and Engineering: C*, 2009, **29**, 1697–1701.
113 R. Massart, *Magnetics, IEEE Transactions on*, 1981, **17**, 1247–1248.
114 C. Blanco-Andujar, D. Ortega, Q. A. Pankhurst and N. T. K. Thanh, *Journal of Materials Chemistry*, 2012, **22**, 12498–12506.
115 T. Sugimoto and E. Matijević, *Journal of Colloid and Interface Science*, 1980, **74**, 227–243.
116 L. Cabrera, S. Gutierrez, N. Menendez, M. P. Morales and P. Herrasti, *Electrochimica Acta*, 2008, **53**, 3436–3441.
117 Y. Piao, J. Kim, H. Na, D. Kim, J. Baek, M. Ko, J. Lee, M. Shokouhimehr and T. Hyeon, *Nature Materials*, 2008, **7**, 242–247.
118 I. Robinson and N. T. K. Thanh, *AIP Conference Proceedings*, 2010, **1275**, 3–12.
119 D. Ung, L. D. Tung, G. Caruntu, D. Delaportas, I. Alexandrou, I. A. Prior and N. T. K. Thanh, *CrystEngComm*, 2009, **11**, 1309–1316.
120 L. T. Lu, L. D. Tung, I. Robinson, D. Ung, B. Tan, J. Long, A. I. Cooper, D. G. Fernig and N. T. K. Thanh, *Journal of Materials Chemistry*, 2008, **18**, 2453–2458.
121 A. Dhawan and V. Sharma, *Anal Bioanal Chem*, 2010, **398**, 589–605.
122 L. Franzel, M. F. Bertino, Z. J. Huba and E. E. Carpenter, *Applied Surface Science*, 2012, **261**, 332–336.
123 C. Yang, R. Jie, L. Jianbo and L. Yan, *Journal of Biomaterials Science, Polymer Edition*, 2011, **22**, 1473–1486.
124 V. M. Khot, A. B. Salunkhe, N. D. Thorat, R. S. Ningthoujam and S. H. Pawar, *Dalton Transactions*, 2013, **42**, 1249–1258.
125 P. Bilalis, A. Chatzipavlidis, L.-A. Tziveleka, N. Boukos and G. Kordas, *Journal of Materials Chemistry*, 2012, **22**, 13451–13454.
126 B. Sivakumar, R. G. Aswathy, Y. Nagaoka, M. Suzuki, T. Fukuda, Y. Yoshida, T. Maekawa and D. N. Sakthikumar, *Langmuir*, 2013, **29**, 3453–3466.
127 S. Brulé, M. Levy, C. Wilhelm, D. Letourneur, F. Gazeau, C. Ménager and C. Le Visage, *Advanced Materials*, 2011, **23**, 787–790.
128 J. L. Arias, V. Gallardo and M. A. Ruiz, In *Methods in Enzymology*, D. Nejat (Ed.), Academic Press, 2012, vol. 508, pp. 61–88.
129 Y. Mi, X. Liu, J. Zhao, J. Ding and S.-S. Feng, *Biomaterials*, 2012, **33**, 7519–7529.
130 W.-H. Chiang, V. T. Ho, H.-H. Chen, W.-C. Huang, Y.-F. Huang, S.-C. Lin, C.-S. Chern and H.-C. Chiu, *Langmuir*, 2013, **29**, 6434–6443.
131 C. Sanson, C. Schatz, J.-F. Le Meins, A. Soum, J. Thévenot, E. Garanger and S. Lecommandoux, *Journal of Controlled Release*, 2010, **147**, 428–435.
132 S.-H. Hu, B.-J. Liao, C.-S. Chiang, P.-J. Chen, I. W. Chen and S.-Y. Chen, *Advanced Materials*, 2012, **24**, 3627–3632.
133 A. E. Smith, X. Xu, D. A. Savin and C. L. McCormick, *Polymer Chemistry*, 2010, **1**, 628–630.
134 M. A. Kosoglu, R. L. Hood, J. H. Rossmeisl, D. C. Grant, Y. Xu, J. L. Robertson, M. N. Rylander and C. G. Rylander, *Lasers in Surgery and Medicine*, 2011, **43**, 914–920.
135 J. McDaniel, M. Dewhirst and A. Chilkoti, *International Journal of Hyperthermia*, 2013, **29**, 501–510.
136 J. R. McDaniel, J. Bhattacharyya, K. B. Vargo, W. Hassouneh, D. A. Hammer and A. Chilkoti, *Angewandte Chemie International Edition*, 2013, **52**, 1683–1687.

137 J. R. McDaniel, S. R. MacEwan, M. Dewhirst and A. Chilkoti, *Journal of Controlled Release*, 2012, **159**, 362–367.
138 Y.-X. J. Wang, *Quantitative Imaging in Medicine and Surgery*, 2011, **1**, 35–40.
139 D. Kim, S. Park, J. H. Lee, Y. Y. Jeong and S. Jon, *Journal of the American Chemical Society*, 2007, **129**, 7661–7665.
140 P.-H. Wang, H.-L. Liu, P.-H. Hsu, C.-Y. Lin, C.-R. Chris Wang, P.-Y. Chen, K.-C. Wei, T.-C. Yen and M.-L. Li, *BIOMEDO*, 2012, **17**, 612221–612225.
141 S. Casciaro, F. Conversano, A. Ragusa, M. Ada Malvindi, R. Franchini, A. Greco, T. Pellegrino and G. Gigli, *Investigative Radiology*, 2010, **45**, 715–724.
142 X. An, F. Zhan and Y. Zhu, *Langmuir*, 2013, **29**, 1061–1068.
143 L. Gao, J. Fei, J. Zhao, H. Li, Y. Cui and J. Li, *ACS Nano*, 2012, **6**, 8030–8040.